Vancomycin dimer formation between analogues of bacterial peptidoglycan surfaces probed by force spectroscopy†

Matthew Batchelor,*‡[a] Dejian Zhou,[b] Matthew A. Cooper,[c] Chris Abell[a] and Trevor Rayment[d]

Received 17th September 2009, Accepted 26th November 2009
First published as an Advance Article on the web 8th January 2010
DOI: 10.1039/b919347b

Functionalised thiols presenting peptides found in the peptidoglycan of vancomycin-sensitive and -resistant bacteria were synthesised and used to form self-assembled monolayers (SAMs) on gold surfaces. This model bacterial cell-wall surface mimic was used to study binding interactions with vancomycin. Force spectroscopy, using the atomic force microscope (AFM), was used to investigate the specific rupture of interfacial vancomycin dimer complexes formed between pairs of vancomycin molecules bound to peptide-coated AFM probe and substrate surfaces. Clear adhesive contacts were observed between the vancomycin-sensitive peptide surfaces when vancomycin was present in solution, and the adhesion force demonstrated a clear dependence on antibiotic concentration.

Introduction

Vancomycin is a powerful antibiotic used to treat infections caused by Gram-positive bacteria. This glycopeptide antibiotic molecule acts by reversibly binding to D-alanyl-D-alanine (DADA) terminating mucopeptides that are present as intermediates in the biosynthesis of bacterial cell-walls. The bound complex contains five specific hydrogen-bonds as well as hydrophobic interactions between the alanine methyl groups and hydrocarbon components of vancomycin (see ESI† Fig. S1 for a binding model).[1] This binding process sterically inhibits the action of cell-wall cross-linking enzymes (transpeptidases and transglycosylases), limiting its growth and thereby preventing microbial growth.[1,2] Research into the properties of vancomycin is currently of particular interest due to its use in the treatment of methicillin-resistant *Staphylococcus aureus* (MRSA) infections, and because of the worrying increase in examples of vancomycin-resistant bacteria,[3,4] which can result from a single amino acid mutation of the terminal D-alanine to D-lactate in the growing bacterial cell-wall.

Many studies have been performed to investigate the interaction of vancomycin with DADA in solution, and on cell-wall mimic surfaces.[5–12] Further studies have shown that vancomycin can form a dimer complex in solution.[13–15] Dimerisation occurs between vancomycin monomers through four hydrogen bonds,[1,16–18] and these interactions occur on the opposite side of the molecule to the site where the DADA ligand binds. The dimerisation constant has been reported to be ~700 M^{-1} in solution.[13] The process of vancomycin dimerisation has been shown to be cooperative with that of vancomycin–DADA binding and it has been suggested that dimerisation plays a role in substrate binding *in vivo* and is important for the overall efficacy of the antibiotic. Furthermore, a synthetic vancomycin dimer has been shown to be more effective against certain vancomycin-resistant organisms than vancomycin alone.[19] To date, all experiments on dimer formation have been performed with solution-phase mimics of mucopeptides, using techniques such as nuclear magnetic resonance (NMR) spectroscopy[13–15,20] and isothermal titration calorimetry (ITC),[21] which may not accurately represent the binding topology found on a bacterial cell surface.

In this study vancomycin dimerisation has been investigated between two antibiotic monomers that are both bound to cell-wall mimic lysyl-D-alanyl-D-alanine (KDADA) surfaces. This represents a novel approach to measuring dimerisation constants, and may prove a useful method to explore the process and effects of dimerisation using a model of a cell-wall system in which interactions are templated on surfaces. The model cell-walls were prepared using the self-assembly of a mixture of functionalised alkanethiols onto gold surfaces. These surfaces were analysed using ellipsometry and contact angle measurements, and surface plasmon resonance (SPR) spectroscopy was used to characterise the binding profiles of vancomycin with surface-bound ligands. Subsequently, force spectroscopy[6,22–24] with the atomic force microscope (AFM) was used to measure directly the force required to rupture the dimer formed between two surface-bound species, as shown schematically in Fig. 1.

Results and discussion

For these studies, gold-coated AFM probes and substrates were functionalised with self-assembled monolayers (SAMs) of peptidic alkanethiols[25] (the molecular structures of the alkanethiols are given in Scheme 1). Mixed SAMs were composed of alkanethiols that contained a tri(ethylene glycol) spacer with a distal KDADA group (**1**), which were diluted with a background of alkanethiols terminating in tri(ethylene glycol)-OH (PEG-OH, **4**).[26] The SAMs

[a]*Department of Chemistry, University of Cambridge, Lensfield Road, Cambridge, UK CB2 1EW. E-mail: m.r.batchelor.98@cantab.net*
[b]*School of Chemistry and the Astbury Centre for Structural Molecular Biology, University of Leeds, Leeds, UK LS2 9JT*
[c]*Institute for Molecular Bioscience, The University of Queensland, Brisbane, 4072, Australia*
[d]*School of Chemistry, University of Birmingham, Birmingham, UK B15 2TT*

† Electronic supplementary information (ESI) available: Binding model and supporting figures; synthesis of compounds and relevant spectra. See DOI: 10.1039/b919347b

‡ Current address: Royal Society of Chemistry, Thomas Graham House, Science Park, Cambridge, UK, CB4 0WF.

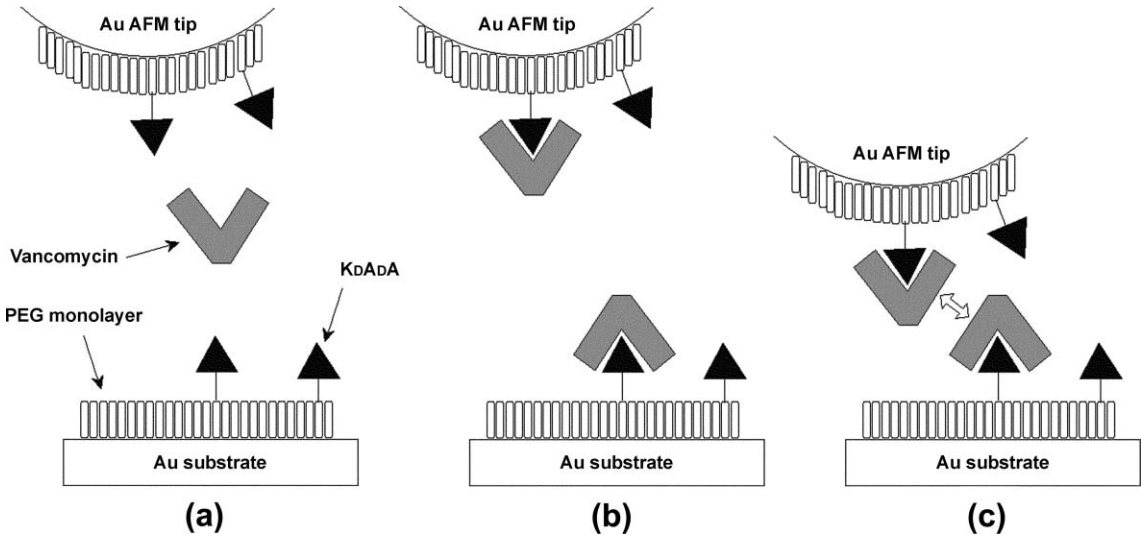

Fig. 1 Schematic for a force spectroscopy investigation of the interacting vancomycin dimer system. (a) KDADA ligands project from the tip and surface. Note: only two KDADA ligands are shown on both the tip and surface for simplicity; the exact number of ligands within the contact region when the tip approaches is likely to be more than shown. The number of ligands depends on the sharpness of the tip, and the contact force used in force spectroscopy collection, and therefore varies for different tip–surface combinations. (b) Vancomycin, added to the intervening solution, binds to ligands on tip and surface. (c) During force spectroscopy measurement, the tip and substrate are pushed together and then pulled apart and the adhesive force between bound vancomycin monomers from the tip and surface is measured.

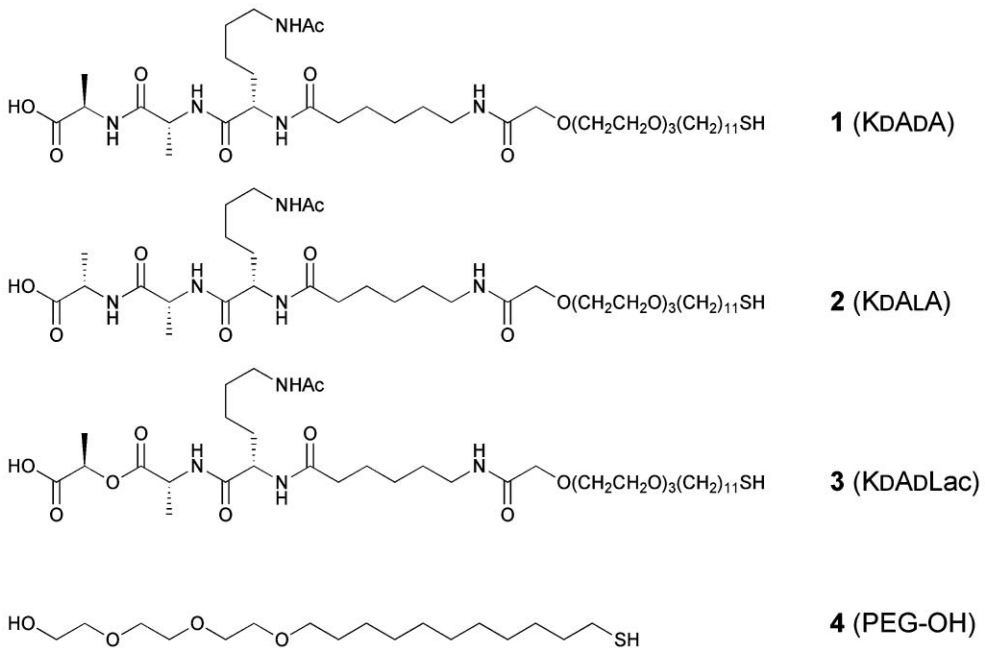

Scheme 1 Molecular structures of functional alkanethiols used in this study.

were formed from a mixed solution of **1** and **4** in a molar ratio of 1 : 9 in ethanol.[5] Alternative peptide-functionalised surfaces were also prepared in an equivalent manner by using alkanethiols with a distal lysyl-D-alanyl-L-alanine (KDALA, **2**) or lysyl-D-alanyl-D-lactate (KDADLac, **3**) group. The surfaces were characterised on flat gold surfaces using ellipsometry (SAM thickness measurements) and water contact angle (CA) goniometry (surface wetting properties)—results are given in Table 1.

The thickness and CA values for the pure PEG-OH monolayer compare very well with those reported in the literature: CA(adv.) 34°, CA(rec.) 22°, thickness 2.0 nm.[27] The small increase in thickness and reduced receding CA change observed when the peptide thiols are present in the monolayer are reasonable given the size and polarity of the peptides. The values obtained were subsequently used as a quality-control for the SAMs used in the spectroscopy measurements.

Table 1 Measured advancing and receding water contact angles (CAs), as well as the ellipsometric thickness, of the pure **4** monolayer, and the peptide-modified monolayers (prepared from a 1 : 9 solution mixture of **1**, **2** or **3** with **4**). Errors represent standard deviations from *n* measurements

SAM	CA(adv.)	CA(rec.)	Thickness/nm
PEG-OH (**4**)	36 ± 1° ($n = 11$)	28 ± 1° ($n = 5$)	2.1 ± 0.3 ($n = 8$)
KDADA (**1**)	35 ± 2° ($n = 7$)	Low/wet ($n = 7$)	2.4 ± 0.5 ($n = 3$)
KDALA (**2**)	34 ± 3° ($n = 4$)	Low/wet ($n = 4$)	2.3 ± 0.4 ($n = 2$)
KDADLac (**3**)	34°	20°	2.4

Further characterisation was achieved by using surface plasmon resonance spectroscopy to monitor the binding behaviour of different concentrations of vancomycin with the surfaces. Examples of typical vancomycin binding profiles are shown in Fig. 2. Scatchard analysis of the equilibrium binding levels (*e.g.* see ESI† Fig. S2) gave a dissociation constant (K_d) of ~0.4 μM, which is consistent with values reported in the literature for both solution[1,10] and surface-phase[5,7] studies. The kinetic behaviour was flow-rate dependent (see ESI† Fig. S3) and, due to the fast inherent on/off-rate of the interaction, accurate rate constants could not be obtained by this technique and the analysis was limited to equilibrium binding levels.[7] Reducing the density of KDADA ligands on the surface resulted in an increase in the observed off-rate and an increase in the K_d determined by Scatchard analysis of equilibrium binding levels. A reduction of the **1** : **4** molar ratio to 1 : 29 gave a K_d of ~1.1 μM—a value that is still in line with the values observed previously, and gives a more accurate lower limit estimate for the dissociation constant for the system used here. Additional control experiments were carried out which showed that the surface-binding behaviour of vancomycin could be blocked by the addition of free acetyl-lysyl-D-alanyl-D-alanine (AcKDADA) to solution (see ESI† Fig. S4). It was also demonstrated that vancomycin did not bind significantly to alternative peptide sequences or to the background surface (*e.g.* ESI† Fig. S5).

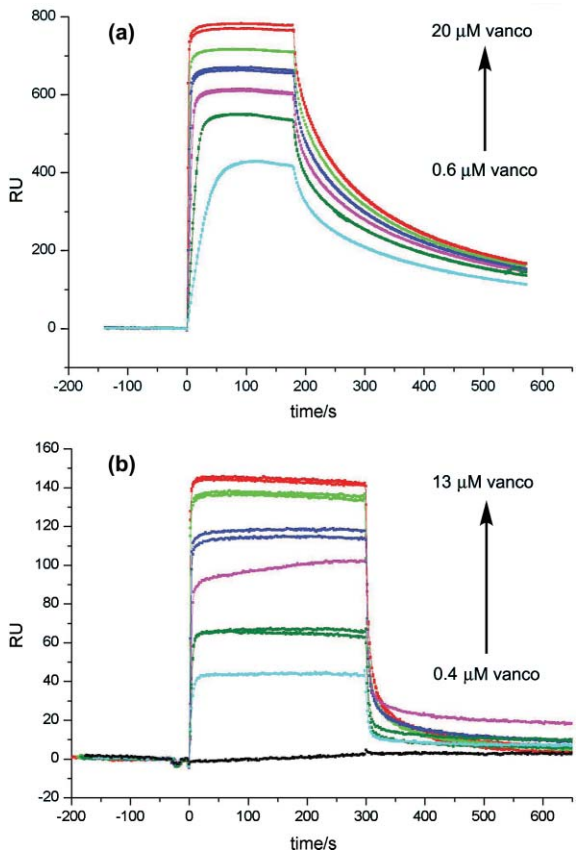

Fig. 2 Overlaid sensorgrams showing typical SPR responses to: (a) 3 min injections of vancomycin at 20 μl min^{-1} across a KDADA chip prepared from a 1 : 9 molar ratio **1** : **4** solution and (b) 5 min injections of vancomycin at 20 μl min^{-1} across a KDADA chip prepared from a 1 : 29 molar ratio **1** : **4** solution (vancomycin concentrations were two-fold dilutions between the values shown; the bottom line in (b) resulted from an injection of buffer).

Force–distance curves were recorded between KDADA-functionalised AFM probes and surfaces in phosphate-buffered saline (PBS) solutions (see Fig. 1 for details about the experimental procedure). No significant adhesion was observed when vancomycin was absent from the solution. The curves all had the appearance of those in Fig. 3a, where approach and retract profiles overlap throughout. When vancomycin (1 μM) was present in the solution the force curves (>90%) showed an enhanced adhesive contact with respect to the above control (see the force curve example in Fig. 3b). Distributions of adhesion forces, recorded using a single probe–surface combination, are shown in Fig. 4. A control experiment with the PBS buffer only represents the measurement of the maximum background noise level (Fig. 4a, average adhesion force ± standard deviation of 43 ± 12 pN). The average adhesion force in 1 μM vancomycin was 180 ± 90 pN. The process was highly reproducible: when the liquid cell was thoroughly rinsed with buffer and the surface-bound vancomycin was washed away, the adhesion force disappeared (Fig. 4c). Re-introduction of vancomycin (1 μM) to the solution again gave an adhesion force of 185 ± 90 pN (Fig. 4d). Several repetitions of this

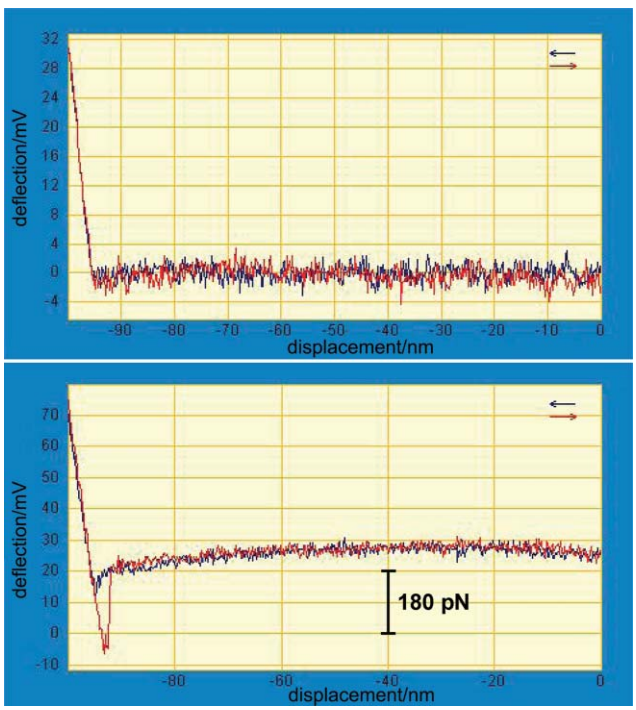

Fig. 3 Raw force–distance curves typical of those recorded between KDADA-functionalised surfaces in buffered solution (top), and in vancomycin-containing buffered solutions (bottom).

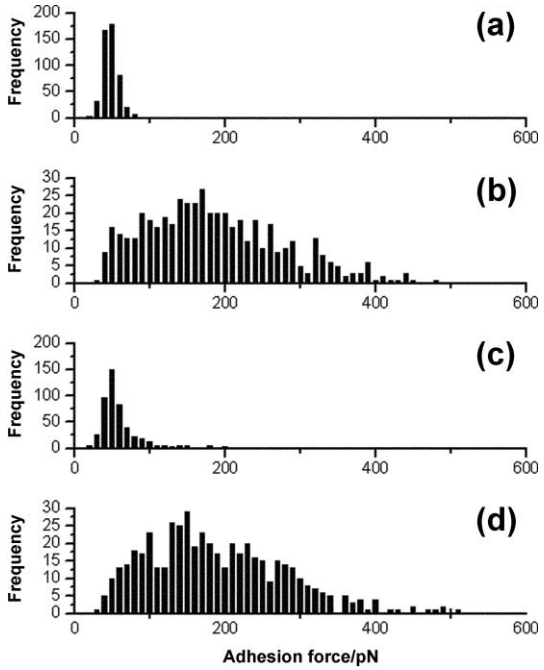

Fig. 4 Histograms showing the adhesion force distributions from ~500 force–distance curves recorded between KDADA-functionalised surfaces (a) in buffer, (b) in 1 μM vancomycin, (c) in buffer after rinsing with buffer, (d) with a regenerated probe surface after introducing 1 μM vancomycin (repeat). The data presented were collected using the same probe–substrate combination. The adhesion values in buffer (~50 pN) correspond to a maximum baseline noise level in the absence of any resolvable adhesion. No effect was observed by altering the histogram bin size.

experiment using different AFM probes and substrates showed similar results, with the average adhesion force ranging from ~150–250 pN, depending on the tip–surface combination used. The same tip–surface combination consistently gave near identical average adhesion forces. This variation in adhesion force between different probes is probably due to differences in the tip radius of the AFM probes, and therefore different numbers of KDADA ligands (and hence bound vancomycin molecules) within the contact region.

To determine if the observed adhesion force was specific to the interaction of vancomycin monomers when bound to KDADA **1**, several control experiments were carried out. Firstly, whilst using the same KDADA-modified tip, the KDADA ligands on the surface were exchanged for alternative peptide sequences KDALA **2** or KDADLac **3**, or the peptide was removed leaving a monolayer of PEG-OH **4** only. Vancomycin is reported to not bind with KDALA,[28] only weakly bind with KDADLac[5] and should not adsorb non-specifically onto the PEG-OH surface.[25] For each of these control surfaces, no adhesion was observed in the presence of 1 μM vancomycin, and the force histograms were similar to those in Fig. 4a and 4c (see ESI† Fig. S6). The average adhesion forces for KDALA, KDADLac and PEG-OH were 47 ± 13 pN, 49 ± 14 pN and 47 ± 14 pN respectively, effectively identical to the background noise level. This control experiment confirmed that the observed adhesion force was highly specific to the KDADA peptide, and strongly suggests that the observed adhesion was indeed due to the formation of inter-surface vancomycin dimers between monomers bound to mucopeptide analogues on the probe and surface. Removal of one partner (*i.e.* the surface monomer) led to complete suppression of the specific adhesion force. In a second control experiment, the tip–surface adhesion between KDADA surfaces in 1 μM vancomycin was completely eliminated by the addition of excess (50 μM) free ACKDADA to the solution (see ESI† Fig. S7). The free ligand effectively competes for and blocks the site that vancomycin would use to bind to the surface, thus greatly reducing the amount of vancomycin on the surface. The process is again reversible, as removal of the free ACKDADA from the system led to the complete recovery of specific adhesive contacts.

Having established that the observed forces were dependent on surface-bound vancomycin, we wished to determine if the system could be used to evaluate surface-templated dimerisation of vancomycin. The adhesion force was observed to be dependent on the concentration of vancomycin in solution (Fig. 5). Both the proportion of recorded curves showing adhesion and the magnitude of adhesion forces measured were affected (representative distributions are given in the ESI† Fig. S8). Few adhesive contacts were observed at low vancomycin concentration (<1 μM). The interactions that were observed were small in magnitude. The largest adhesion forces occurred at ~10 μM vancomycin, and nearly all curves collected showed an adhesive interaction. Above 10 μM, the number and the magnitude of adhesive forces observed were reduced.

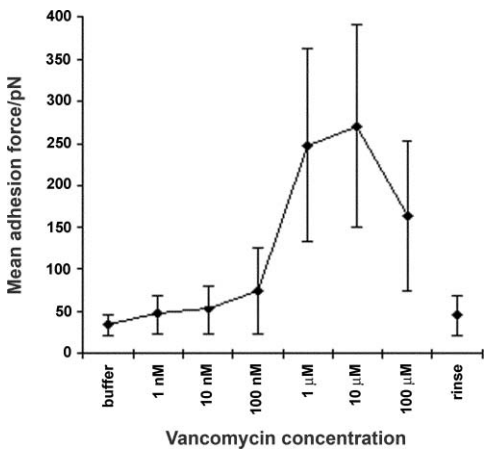

Fig. 5 A plot of the average adhesion forces from ~500 force–distance curves for increasing concentrations of vancomycin in solution. The data presented were collected using the same probe–substrate combination; repeat experiments showed the same trend. The initial sigmoidal response is followed by a reduction in adhesion at high concentration. Rinsing the surfaces with buffer resulted in the loss of adhesive contacts. Error bars show the standard deviation for each distribution.

Below the K_d for vancomycin–KDADA binding, found to be around 1 μM here and in previous solution and surface-based studies,[1,5,7,10] relatively few vancomycin molecules will be bound to ligands on the probe and surface. Thus the likelihood of a bound vancomycin molecule on the tip interacting with another bound molecule on the surface to form an inter-surface dimer is low, and hence there is no concomitant increase in adhesion forces. The amount of vancomycin bound to both surfaces will have increased until all the accessible sites were occupied as the concentration rose above the K_d (*e.g.* at about ten times the K_d, 90%

of the available binding sites would be occupied). As the surfaces were pushed together, the likelihood of an interaction being observed between vancomycin molecules bound to the tip and surface greatly increased, leading to the observed maximum adhesion force. The subsequent reduction in average adhesion force observed at even higher vancomycin concentrations may be attributed to the introduction of a population of dimers bound to either of the surfaces (*i.e.* 'on-surface' dimers which form when ligand-bound vancomycin binds a free vancomycin molecule from solution, see Fig. 6a) prior to the force spectroscopy measurement. The number of sites for inter-surface dimers (between the tip and surface) to form would be reduced, leading to reduced adhesion forces. A recent study has shown that, at higher vancomycin concentrations than used here, ligand-mediated supramolecular complexes can form through alternative dimerisation modes. This could also be a factor influencing the adhesion levels observed at 100 μM.[18]

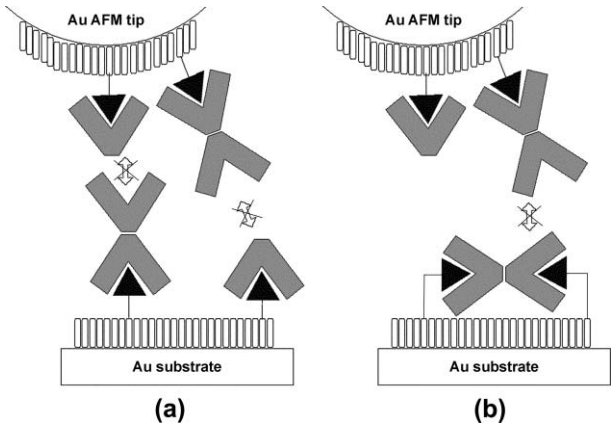

Fig. 6 Schematics showing the possible reasons behind the decreased adhesion force at high vancomycin concentrations. (a) The formation of 'on-surface' dimers between ligand-bound vancomycins and free vancomycin molecules from solution; (b) 'intra-surface' dimers from two neighbouring ligand-bound vancomycin molecules on the same surface (can equally happen on the tip). Both could prevent the formation of 'inter-surface' dimers between monomers bound on tip and surface, and therefore decrease the adhesion force. We believe the major contribution for the adhesion decrease at high vancomycin concentration is due to (a) rather than (b), as (b) is less dependent on vancomycin concentration.

These data suggest that most of the interactions observed in these studies were from the breakage of more than one dimer interaction. At micromolar concentrations nearly all the curves collected displayed a specific interaction. Poisson distribution statistics indicate that, given this feature, the observation of a single-molecule interaction is less probable than that of multiple interactions. This is supported by the correlation between smaller adhesion forces and reduced number of adhesive interactions in proportion to the total number of curves collected. It is possible that single-molecule interactions occur at forces on the cusp of the resolution of the system.

Conclusion

In summary, cell-wall mimic KDADA-presenting surfaces were prepared by using self-assembled monolayers of functional KDADA-terminating thiols on gold, and the vancomycin–surface binding properties were characterised using SPR. Using force spectroscopy with an AFM, clear adhesive contacts were observed between two of these KDADA surfaces when vancomycin was present in solution. The adhesion was dependent upon the concentration of vancomycin and specific to KDADA. We attribute the adhesion force to the breakage of vancomycin dimers which form a bridge between the two KDADA surfaces. The adhesion showed a dependence on concentration that initially followed the thermodynamics of vancomycin–KDADA binding, but at high vancomycin concentrations a significant reduction of adhesion was observed. The dimerisation constants[13,21] for vancomycin are reported to be $K_{dim} < 700$ M^{-1} in solution, and therefore high proportions of dimers are only expected to form at concentrations above ~1.4 mM. However, it has previously been shown that when DADA ligands are present in solution the dimerisation constant is increased by about a factor of ten.[15,20,21] The significant decrease in adhesion shown at 100 μM agrees well with these earlier observations, and our results are therefore a further indication of the cooperative nature of ligand binding and dimerisation. Whilst more detailed investigation would be necessary, it is possible that cooperativity could be further enhanced in our case because, when ligands are fixed on a surface or in a growing cell-wall, the close proximity of neighbouring surface ligands could reduce the entropic penalty for dimer formation between a pair of ligand-bound vancomycin monomers at neighbouring surfaces (see the possible intra-surface dimer model in Fig. 6b).

By using the intimate proximity of the modified AFM tip and substrate, the system can approximate the neighbouring mucopeptides in a growing cell-wall surface. It therefore represents an improved model system (compared to purely solution-based methods) for studying the formation and/or disruption of dimer complexes of this type. The method could allow direct investigation into the relationship between dimer formation and ligand binding. Improving the force resolution, through use of an AFM with lower thermal noise, using sharper tips and reducing the ligand surface density, would allow the investigation of energy barriers for single-dimer interactions through dynamic force spectroscopy, and more generally, this approach could be used to give greater insight into the behaviour of species exhibiting bivalent binding interactions, including investigations into the feature of cooperativity.

Experimental

Materials

Buffer constituents, vancomycin and AcKDADA were from Sigma (and used as received). Deionised water (18.2 MΩ cm at source; Millipore, USA) was used throughout. The synthesis of the 11-mercaptoundecyl tri(ethylene glycol) alcohol (**4**) has been described previously.[26] The KDADA-modified thiol (**1**) was synthesized by solid phase methodology under argon using a commercially available Wang resin and standard Fmoc-protecting group chemistry (see ESI† Scheme S2). The cleaved product was further purified by reverse phase high performance liquid chromatography (HPLC) on a C_{18} column by varying the mobile phase from 5% to 95% of acetonitrile in water (with 0.5% trifluoroacetic acid). The peptide-modified thiols **2** (KDALA) and

3 (KDADLac) were prepared by similar methods. A description of the synthesis of the thiol-protected carboxylic acid[7] (compound **5**), used in the preparation of the peptide thiols, is given in the ESI† Scheme S1. The peptide-thiols (**1–3**) and PEG-OH (**4**) were characterized by NMR and high resolution mass spectrometry (HRMS, +ESI, Q-TOF) as follows:

1 (KDADA). ^{1}H NMR (δ ppm, 400 MHz, CD_3OD): 1.25–1.80 (m, 36H, [15CH_2 + 2CH_3]), 1.91 (s, 3H, CH_3), 2.24 (t, 2H, CH_2), 2.47 (t, 2H, J = 7.1 Hz, CH_2SH), 3.14 (t, 2H, J = 7.0 Hz, NHCH_2), 3.22 (t, J = 7.0 Hz, 2H, NHCH_2), 3.44 (t, 2H, J = 6.7 Hz, -CH_2(OEG)-), 3.54–3.69 (m, 12H, 3(EG)), 3.96 (s, 2H, OCH_2C=O), 4.21 (t, 1H, J = 7.1 Hz, L-Lys-α-CH), 4.31–4.42 (m, 2H, 2 [D-Ala-α-CH]). ^{13}C NMR (δ ppm, 125 MHz, $CDCl_3$): 176.24, 175.58, 174.46, 174.29, 173.21, 172.61 (6 *C*=O), 72.39, 71.95, 71.55, 71.52, 71.37, 71.22, 71.16 (PEG), 55.15, 50.00, 40.17, 39.83, 36.50, 35.22, 32.27, 30.72, 30.70, 30.64, 30.56, 30.27, 30.21, 29.40, 27.57, 27.21, 26.46, 24.97, 24.23, 22.57, 18.01, 17.50. HRMS (+ESI, Q-TOF), found 842.4941; required for $C_{39}H_{73}N_5O_{11}SNa$ [M + Na]$^+$, 842.4925, dev. 1.86 ppm.

2 (KDALA). ^{1}H NMR (δ ppm, 400 MHz, CD_3OD): 1.25–1.80 (m, 36H, [15CH_2 + 2CH_3]), 1.91 (s, 3H, CH_3), 2.24 (t, 2H, J = 7.2 Hz, CH_2), 2.47 (t, 2H, J = 7.1 Hz, CH_2SH), 3.15 (t, 2H, J = 7.0 Hz, NHCH_2), 3.22 (t, J = 7.0 Hz, 2H, NHCH_2), 3.45 (t, 2H, J = 7.0 Hz, -CH_2(OEG)-), 3.54–3.67 (m, 12H, 3(EG)), 3.96 (s, 2H, OCH_2C=O), 4.14 (t, 1H, J = 7.1 Hz, L-Lys-α-CH), 4.31-4.40 (m, 2H, 2 [Ala-α-CH]). ^{13}C NMR (δ ppm, 125 MHz, $CDCl_3$): 176.22, 175.83, 174.67, 174.44, 173.21, 172.62 (6 *C*=O), 72.39, 71.96, 71.57, 71.53, 71.39, 71.22, 71.18 (PEG), 55.52, 50.24, 40.16, 39.82, 36.39, 35.24, 32.00, 30.74, 30.72, 30.65, 30.58, 30.28, 30.22, 30.06, 29.41, 27.58, 27.22, 26.45, 24.97, 24.28, 22.57, 17.93, 17.60. HRMS (+ESI, Q-TOF), found 842.4916; required for $C_{39}H_{73}N_5O_{11}SNa$ [M + Na]$^+$, 842.4925, dev. –1.11 ppm.

3 (KDADLac). ^{1}H NMR (δ ppm, 500 MHz, CD_3OD): 1.25–1.80 (m, 36H, [15CH_2 + 2CH_3]), 1.92 (s, 3H, CH_3), 2.24 (t, 2H, J = 7.0 Hz, CH_2), 2.47 (t, 2H, J = 7.0 Hz, CH_2SH), 3.13–3.17 (m, 2H, NHCH_2), 3.18–3.24 (m, 2H, NHCH_2), 3.46 (t, 2H, J = 6.7 Hz, -CH_2(OEG)), 3.55–3.68 (m, 12H, 3(EG)), 3.96 (s, 2H, OCH_2C=O), 4.30–4.40 (m, 1H, L-Lys-α-CH), 4.40–4.50 (m, 1H, D-Ala-α-CH]). 5.00-5.10 (m, 1H, D-Lac-α-CH). ^{13}C NMR (δ ppm, 125 MHz, CD_3OD): 175.99, 174.12, 173.34, 173.20, 172.84, 172.60 (6 *C*=O), 79.47, 72.40, 71.99, 71.58, 71.55, 71.39, 71.24, 71.19 (PEG), 54.37, 53.68, 40.19, 39.82, 36.73, 36.63, 35.23, 32.84, 32.22, 30.74, 30.71, 30.64, 30.57, 30.26, 30.21, 30.00, 29.85, 29.41, 27.58, 27.52, 27.22, 26.62, 26.56, 24.98, 24.17, 22.60 (*C*H_3), 17.51 (*C*H_3), 17.44 (*C*H_3). HRMS (+ESI, Q-TOF), found 843.4761; required for $C_{39}H_{73}N_5O_{11}SNa$ [M + Na]$^+$, 843.4765, dev. –0.53 ppm.

4 (PEG-OH). ^{1}H NMR (250 MHz, $CDCl_3$, δ ppm): 1.20–1.37 (m, 14H, 7CH_2), 1.49–1.60 (m, 4H, 2CH_2), 2.46 (q, 2H, J = 7.0 Hz, HSCH_2-), 3.05 (s, br, 1H, -OH), 3.40 (t, 2H, J = 7.0 Hz, -CH_2PEG), 3.50–3.75 (m, 12H, 3(OCH_2CH_2). ^{13}C NMR (62.5 MHz, $CDCl_3$, δ ppm): 72.5, 71.4, 70.5, 70.3, 69.9, 61.5, 34.0, 33.7, 30.5, 29.5, 29.4, 29.0, 28.8, 28.7, 28.3, 26.0, 24.5. HRMS (Q-TOF, ES$^+$), found 359.2222; required for $C_{17}H_{36}O_4SNa$ [M + Na]$^+$, 359.2232.

Solutions were prepared in absolute ethanol at a total thiol concentration of 1 mM, and a 1 : 9 mixture of **1** and **4** (or **2**/**3** and **4**) was used for the preparation of mixed SAMs. All experiments were performed in PBS (10 mM sodium phosphate, 138 mM NaCl, 2.7 mM KCl, pH 7.4). Solutions were passed through a 0.2 μm syringe filter before use (Whatman, USA).

Monolayer characterisation

SAMs were characterised on thick thermally-evaporated gold on silicon samples using water contact angle and ellipsometry measurements. Thickness measurements were performed with an EL X-02C High Precision Ellipsometer (DRE, Germany). Δ and Ψ measurements were recorded for five sites on bare gold substrates, and a two-layer model, based on the average values, was used to calculate the refractive index of the substrate. Further Δ and Ψ measurements were then taken on the gold substrates after they had been incubated for at least 18 h in solutions containing the appropriate mixture of alkanethiols (the samples being thoroughly rinsed in ethanol and dried under nitrogen before measurements recorded). The refractive index of the gold, and an assumed organic refractive index of 1.45 were used in a three-layer model to calculate the thickness of the SAM. Thickness values were calculated for measurements at 5 sites on each sample. No account was made for different functional tailgroups.

For contact angle measurements, a motorised syringe with needle was fixed above the sample on an adjustable stage. Milli-Q de-ionised water was added to, or removed from the SAM-covered sample surface without removing the needle from the droplet (method B, Bain *et al.*[29]). A CCD camera positioned at sample level and perpendicular to the syringe was used to record images. Advancing contact angles were recorded when the edge of the droplet was seen to extend across the surface, and receding contact angles when the periphery began to shrink. Measurements of the contact angles were individually performed, by hand, for both the left and right sides of the droplet using Scion Image (Frederick, MD, USA). Reported values are the average of left and right sides and n different samples. Contact angles were also recorded, with similar results, on the gold-on-mica samples used in force spectroscopy measurements.

Surface plasmon resonance spectroscopy

SPR spectroscopy studies were performed using a Biacore-X instrument (Biacore, Sweden). Gold-coated chips were purchased from Biacore (SIA Kit Au) and prior to use were cleaned for 1–2 min in freshly prepared piranha solution. After extensive rinsing with deionised water, the chips were dried with nitrogen gas and placed into the appropriate thiol solution for at least 18 h. After this incubation period, the chips were thoroughly rinsed with ethanol and then with water, before mounting and docking in the instrument. PBS was used as running buffer, using a fixed flow rate, generally at 10 or 20 μl min^{-1}. The chips were exposed to 3–5 min injections of vancomycin in PBS. Before each vancomycin injection the surface was regenerated using 10–20 μl of 10 mM NaOH and the chip was exposed to flowing buffer until a stable baseline was achieved. All SPR experiments were performed at 25 °C.

Preparation of tips and surfaces

Mica sheets (Agar Scientific, UK) were cut into 1 cm^2 pieces and then cleaved. AFM probes (DNP-S, Veeco, nominal k = 60 pN

nm^{-1}) were used as received. The probes and cleaved mica were placed into an Edwards Auto 500 vacuum coater, and 5 nm of chromium (Testbourne Ltd, UK, 99.99%) followed by 30–35 nm of gold (Birmingham Metal, UK, 99.99%) were deposited by thermal evaporation. Upon removal, the gold substrates were immediately placed into the appropriate thiol solution and left for at least 18 h. Before use the substrates were thoroughly rinsed with ethanol and dried under nitrogen.

Force spectroscopy

Force measurements were performed using a Dimension 3100 AFM with a Nanoscope IV controller (Veeco, USA). Equilibration times of 30 min in PBS solution were generally required to produce a steady laser signal. 500 force–distance curves were recorded, over different areas of the surface, for each sample or solution change. Each curve was measured over a 100 nm range at a rate of 1 Hz (200 nm s^{-1}) and the maximum loading force was maintained at a low level (a few 100 pN). Cantilever spring constants were calibrated *ex situ* using the routines of an MFP-1D (Asylum Research, USA), which utilises the thermal resonance method.[30] Values were typically 100–120 pN nm^{-1}. Force–distance curves were then analysed using the Scanning Probe Image Processor (Image Metrology, Denmark).

References

1 D. H. Williams and B. Bardsley, *Angew. Chem., Int. Ed.*, 1999, **38**, 1172–1193.
2 K. C. Nicolaou, C. N. C. Boddy, S. Brase and N. Winssinger, *Angew. Chem., Int. Ed.*, 1999, **38**, 2096–2152.
3 L. B. Rice, *Emerging Infect. Dis.*, 2001, **7**, 183–187.
4 F. C. Tenover, J. W. Biddle and M. V. Lancaster, *Emerging Infect. Dis.*, 2001, **7**, 327–332.
5 M. A. Cooper, M. T. Fiorini, C. Abell and D. H. Williams, *Bioorg. Med. Chem.*, 2000, **8**, 2609–2616.
6 Y. Gilbert, M. Deghorain, L. Wang, B. Xu, P. D. Pollheimer, H. J. Gruber, J. Errington, B. Hallet, X. Haulot, C. Verbelen, P. Hols and Y. F. Dufrene, *Nano Lett.*, 2007, **7**, 796–801.
7 J. Lahiri, L. Isaacs, J. Tien and G. M. Whitesides, *Anal. Chem.*, 1999, **71**, 777–790.
8 D. H. Williams, *Nat. Prod. Rep.*, 1996, **13**, 469–477.
9 P. H. Popieniek and R. F. Pratt, *J. Am. Chem. Soc.*, 1991, **113**, 2264–2270.
10 M. Nieto and H. R. Perkins, *Biochem. J.*, 1971, **123**, 773–787.
11 H. R. Perkins, *Biochem. J.*, 1969, **111**, 195–205.
12 J. Ndieyira, M. Watari, A. D. Barrera, D. Zhou, M. Vogtli, M. Batchelor, M. A. Cooper, T. Strunz, M. A. Horton, C. Abell, T. Rayment, G. Aeppli and R. A. McKendry, *Nat. Nanotechnol.*, 2008, **3**, 691–696.
13 U. Gerhard, J. P. Mackay, R. A. Maplestone and D. H. Williams, *J. Am. Chem. Soc.*, 1993, **115**, 232–237.
14 J. P. Mackay, U. Gerhard, D. A. Beauregard, R. A. Maplestone and D. H. Williams, *J. Am. Chem. Soc.*, 1994, **116**, 4573–4580.
15 J. P. Mackay, U. Gerhard, D. A. Beauregard, M. S. Westwell, M. S. Searle and D. H. Williams, *J. Am. Chem. Soc.*, 1994, **116**, 4581–4590.
16 M. Schäfer, T. R. Schneider and G. M. Sheldrick, *Structure*, 1996, **4**, 1509–1515.
17 P. J. Loll, A. E. Bevivino, B. D. Korty and P. H. Axelsen, *J. Am. Chem. Soc.*, 1997, **119**, 1516–1522.
18 P. J. Loll, A. Derhovanessian, M. V. Shapovalov, J. Kaplan, L. Yang and P. H. Axelsen, *J. Mol. Biol.*, 2009, **385**, 200–211.
19 U. N. Sundram, J. H. Griffin and T. I. Nicas, *J. Am. Chem. Soc.*, 1996, **118**, 13107–13108.
20 D. H. Williams, A. J. Maguire, W. Tsuzuki and M. S. Westwell, *Science*, 1998, **280**, 711–714.
21 D. McPhail and A. Cooper, *J. Chem. Soc., Faraday Trans.*, 1997, **93**, 2283–2289.
22 A. Janshoff, M. Neitzert, Y. Oberdorfer and H. Fuchs, *Angew. Chem., Int. Ed.*, 2000, **39**, 3212–3237.
23 R. McKendry, M. E. Theoclitou, T. Rayment and C. Abell, *Nature*, 1998, **391**, 566–568.
24 X. Z. Wang, D. J. Zhou, K. Sinniah, C. Clarke, L. Birch, H. T. Li, T. Rayment and C. Abell, *Langmuir*, 2006, **22**, 887–892.
25 K. L. Prime and G. M. Whitesides, *J. Am. Chem. Soc.*, 1993, **115**, 10714–10721.
26 D. J. Zhou, L. M. Ying, X. Hong, E. A. Hall, C. Abell and D. Klenerman, *Langmuir*, 2008, **24**, 1659–1664.
27 C. Pale-Grosdemange, E. S. Simon, K. L. Prime and G. M. Whitesides, *J. Am. Chem. Soc.*, 1991, **113**, 12–20.
28 M. Nieto and H. R. Perkins, *Biochem. J.*, 1971, **123**, 789–803.
29 C. D. Bain, E. B. Troughton, Y. T. Tao, J. Evall, G. M. Whitesides and R. G. Nuzzo, *J. Am. Chem. Soc.*, 1989, **111**, 321–335.
30 J. L. Hutter and J. Bechhoefer, *Rev. Sci. Instrum.*, 1993, **64**, 1868–1873.

